RESEARCH ARTICLE

Evolutionary engineering and transcriptomic analysis of nickel-resistant *Saccharomyces cerevisiae*

Gökhan Küçükgöze[1,2], Ceren Alkım[1,2], Ülkü Yılmaz[1,2], H. İbrahim Kısakesen[1,2,3], Sema Gündüz[4], Süleyman Akman[4] & Z. Petek Çakar[1,2]

[1]Department of Molecular Biology & Genetics, Faculty of Science & Letters, Istanbul Technical University, Maslak, Istanbul, Turkey; [2]Istanbul Technical University, Dr. Orhan Öcalgiray Molecular Biology, Biotechnology and Genetics Research Center (ITU-MOBGAM), Maslak, Istanbul, Turkey; [3]SEM Lab A.Ş., Istanbul, Turkey; and [4]Department of Chemistry, Faculty of Science & Letters, Istanbul Technical University, Maslak, Istanbul, Turkey

Correspondence: Zeynep P. Çakar, Department of Molecular Biology & Genetics, Faculty of Science & Letters, Istanbul Technical University, Maslak, Istanbul 34469, Turkey. Tel.: +90 212 285 72 63; fax: +90 212 285 63 86; e-mail: cakarp@itu.edu.tr

Received 22 April 2013; revised 23 July 2013; accepted 22 August 2013.
Final version published online 3 October 2013.

DOI: 10.1111/1567-1364.12073

Editor: Jens Nielsen

Keywords
evolutionary engineering; inverse metabolic engineering; yeast DNA microarray analysis; nickel resistance; *Saccharomyces cerevisiae*; stress resistance.

Note: This work is fully MIAME-compliant and has been deposited at GEO Website. The accession number is GSE50985 at http://www.ncbi.nlm.nih.gov/geo/query/acc.cgi?acc=GSE50985

Abstract

Increased exposure to nickel compounds and alloys due to industrial development has resulted in nickel pollution and many pathological effects on human health. However, there is very limited information about nickel response, transport, and tolerance in eukaryotes. To investigate nickel resistance in the model eukaryote *Saccharomyces cerevisiae*, evolutionary engineering by batch selection under gradually increasing nickel stress levels was performed. Nickel hyper-resistant mutants that could resist up to 5.3 mM $NiCl_2$, a lethal level for the reference strain, were selected. The mutants were also cross-resistant against iron, cobalt, zinc, and manganese stresses and accumulated more than twofold higher nickel than the reference strain. Global transcriptomic analysis revealed that 640 upregulated genes were related to iron homeostasis, stress response, and oxidative damage, implying that nickel resistance may share common mechanisms with iron and cobalt resistance, general stress response, and oxidative damage.

Introduction

Nickel is an industrially important element, which belongs to the transition metal group in the periodic table of elements. It is a widely distributed element in the environment and is derived from either natural sources or anthropogenic activities. Nickel in ambient air is derived from volcanic emissions, forest fires, combustion of coal and oil, and mining and refining of nickel ores. Nickel is also present in water, due to the leaching of nickel compounds from soil, as well as sedimentation or disposal of nickel compounds and ores (Cempel & Nikel, 2006). As a transition metal, nickel is heat and corrosion-resistant and is therefore widely used in the production of stainless steel tools and appliances. Nickel alloys are also used in the production of nickel–cadmium batteries, electronic equipment, jewelry, medical prostheses, and casting coins (Denkhaus & Salnikow, 2002; Reck *et al.*, 2008).

Industrial development has led to an increase in the exposure to nickel compounds and alloys, which in turn have led to a variety of pathological effects on human health, such as lung and nasal cancers, as well as cardiovascular and kidney diseases. Additionally, skin contact with nickel compounds can result in allergic dermatitis (Kasprzak *et al.*, 2003). High nickel concentrations can also be

very toxic to microorganisms as they cause alterations in the composition of macromolecules such as DNA and proteins. Toxicity also occurs due to the alteration in carbohydrate metabolism and organic ions, because nickel ions can interfere with other metal ions such as magnesium and iron. Additionally, nickel damages lipid membranes, resulting in the excretion of pyruvate and potassium ions from the cell (Joho *et al.*, 1995). Thus far, nine nickel-dependent enzymes have been identified in bacteria, archaea, fungi, algae, and higher plants (reviewed by Mulrooney & Hausinger, 2003).

Studies on the mechanism of nickel transport in bacteria have revealed the existence of two major types of nickel uptake mechanisms: ATP-binding cassette transporter systems and nickel-specific permeases. In eukaryotes, nickel transport mechanisms are not well understood, and any homolog of these bacterial transporters has not been reported in the model eukaryotic microorganism *Saccharomyces cerevisiae* (Eitinger & Mandrand-Berthelot, 2000). Concerning the molecular mechanism of nickel uptake in *S. cerevisiae,* it was suggested that nickel ions are transported into the vacuole by a proton-gradient-driven system (Nishimura *et al.*, 1998). It was reported that a nickel-resistant mutant of *S. cerevisiae* accumulated more than 70% of the internal nickel ions in the vacuolar fractions. It was also shown that intact vacuoles without any mutation to disrupt vacuolar biogenesis and function are necessary for nickel accumulation (Eide *et al.*, 2005). Authors also estimated large amounts of histidine in the vacuole and suggested the possible role of histidine–nickel complexes in the sequestration of internal nickel ions into the vacuoles (Joho *et al.*, 1992). In another study, a histidine auxotrophic strain showed alleviated nickel tolerance when the medium was supplemented with L-histidine (Farcasanu *et al.*, 2005). However, uptake of nickel ions into the cytoplasm remains unclear. On the other hand, Nic1p of the fission yeast *Schizosaccharomyces pombe* is a high-affinity nickel permease and the first example of this kind of transporter in a eukaryotic organism. *nic1*Δ mutants of *S. pombe* were unable to utilize urea as a nitrogen source and showed reduced nickel accumulation compared with the parental strain (Eitinger *et al.*, 2000).

Evolutionary engineering is based on the systematic application of a selection procedure to obtain a desired phenotype (Butler *et al.*, 1996; Sauer, 2001). Unlike rational metabolic engineering, this approach does not require preliminary knowledge about the genetic or biochemical basis of a desired phenotype. For this reason, it is mainly used for strain improvement and investigating molecular mechanisms of genetically complex phenotypes such as stress resistance (Nevoigt, 2008; Çakar *et al.*, 2012). In the literature, there are successful examples of evolutionary engineering including improved resistance toward cobalt (Çakar *et al.*, 2009), isobutanol (Minty *et al.*, 2011), boron (Şen *et al.*, 2011), multiple stresses (Çakar *et al.*, 2005), and ethanol fermentation using mixed substrates (xylose and arabinose) (Wisselink *et al.*, 2009) and lactose (Guimaraes *et al.*, 2008).

The aim of this study was to obtain nickel-resistant *S. cerevisiae* mutants by evolutionary engineering and perform the phenotypic and transcriptomic analysis of the mutants to investigate nickel resistance in *S. cerevisiae*. Nickel-resistant mutants were obtained by continuously applying nickel stress to a chemically mutagenized *S. cerevisiae* culture, by gradually increasing nickel stress level at each repetitive batch culture. Nickel-resistant individual mutants were randomly selected from the final mutant population, and their potential cross-resistances to other metal and nonmetal stresses were determined. One of the highly nickel-resistant mutants, M9, was chosen for detailed physiological characterization and determination of its cellular nickel contents. Finally, comparative transcriptomic analyses of the reference strain and the nickel-resistant mutant, M9, were performed to gain insight into the transcriptomic changes that may be linked to nickel resistance in *S. cerevisiae*.

Materials and methods

Strain, media, growth, and storage conditions

In this study, *S. cerevisiae* strain CEN.PK 113-7D (*MATa*, *MAL2-8*^{c}, *SUC2*) as described by Entian & Kötter (2007) was used as the reference strain. It was kindly provided by Dr. Laurent Benbadis (INSA-Toulouse, France). Yeast minimal medium 'YMM' [2% w/v glucose, 0.67% w/v yeast nitrogen base without amino acids (Difco)] and yeast peptone dextrose medium 'YPD' (1% w/v peptone, 1% w/v yeast extract, 2% w/v glucose) were used as culture media. Cultures were grown at 30 °C and 150 r.p.m., using 50-mL culture tubes containing 10 mL YMM. Cell growth was monitored by measuring the optical density at 600 nm ($OD_{600\ nm}$) using a Shimadzu UV-1700 (Japan) spectrophotometer. Cultures were stored as 2 mL suspensions at −80 °C in YMM containing 30% (v/v) glycerol.

Evolutionary engineering strategy for selection of nickel-resistant yeast mutants

To obtain nickel-resistant *S. cerevisiae* mutants, an evolutionary engineering strategy similar to our previous selection procedure for cobalt-resistant *S. cerevisiae* (Çakar *et al.*, 2009) was employed. To increase the genetic diversity of the initial population for selection, ethyl methane sulfonate mutagenesis (EMS) was applied to the reference strain (Lawrence, 1991; Çakar *et al.*, 2009), such that 10%

of the initial culture survived the mutagenesis procedure. The minimum inhibitory concentration (MIC) for nickel that causes 50% growth reduction was determined for both reference strain and the EMS-mutagenized starting population for selection. The $NiCl_2$ concentrations used in this screening test varied from 0.05 to 1 mM.

The selection strategy involved successive batch cultivation of the EMS-mutagenized culture in the presence of $NiCl_2$ stress, which varied between 0.05 and 5.3 mM and was gradually increased between each successive passage. Initially, the EMS-mutagenized culture was inoculated into 10 mL of YMM containing 0.05 mM $NiCl_2$. Upon 24 h of cultivation, the culture was centrifuged at 10 000 ***g*** for 5 min using a benchtop centrifuge (Eppendorf, Centrifuge 5424, Germany), washed twice with fresh YMM, and inoculated into fresh YMM containing $NiCl_2$ at an initial $OD_{600\ nm}$ of 0.2 in 10 mL culture volume. The culture that grew in the presence of 0.05 mM $NiCl_2$ was named as the first passage. The second passage was obtained by exposing the first passage to 0.1 mM $NiCl_2$ in YMM. For each passage, an aliquot of 2 mL yeast culture was washed twice with YMM and stored at −80 °C in 30% (v/v) glycerol. At every successive passage, $NiCl_2$ concentrations were increased by 0.05 mM up to 2.45 mM $NiCl_2$ concentration. Beyond that, nickel concentrations were increased more rapidly for 10 more passages, until a final $NiCl_2$ concentration of 5.3 mM. At this level, the selection experiment was stopped, and mutant individuals were selected from the final population by growing it on solid YMM plates by serial dilution and randomly isolating colonies as mutant individuals.

Stress resistance estimation

Resistance against nickel and a variety of stress conditions was determined using a high-throughput, most probable number (MPN) assay (Russek & Colwell, 1983), as well as by spotting assay, that is, serial dilutions on solid culture media. For spotting assay, precultures of yeast cells were grown overnight at 30 °C in 10 mL YMM until they reached late log phase. Culture volume that corresponded to 4 $OD_{600\ nm}$ units in 1 mL volume was collected by centrifugation. The culture was serially diluted by fourfold, and 2.5 μL from the samples was spotted onto solid YMM containing 0.15–5 mM $NiCl_2$ (Merck, Germany), 5 mM $CoCl_2$ (Fluka), 50 mM $(NH_4)_2Fe(SO_4)_2$ (Merck, Germany), 20 mM $MnCl_2$ (Sigma), 10 mM $ZnCl_2$ (Sigma ALDRICH), 0.5 M $MgCl_2$ (Merck, Germany), 0.1 mM $CuSO_4$ (Sigma ALDRICH), 1 mM H_2O_2 (Merck, Germany), 8% (v/v) ethanol (J.T. Baker, the Netherlands), 0.5 M NaCl (Carlo Erba, Italy), and 160 μM BPS (Sigma), as well as on YMM plates as control group and grown at 30 °C for 48 h.

Viable cell numbers were determined by serial dilutions in 96-well plates containing 180 μL YMM. Dilutions were made in the range of 10^{-1}–10^{-8} as five parallel repeats. The MPN of survivors was estimated using published MPN tables based on the ability of yeast cells to grow at higher dilutions. For this purpose, cells were grown in YMM containing $NiCl_2$ (0.15 and 3.5 mM), $CoCl_2$ (2.5 mM), $(NH_4)_2Fe(SO_4)_2$ (30 mM), $MnCl_2$ (20 mM), and $ZnCl_2$ (10 mM) for 72 h. Based on visual inspection of each well for growth, MPN scores were determined, and viable cell numbers were estimated using MPN tables (http://www.jlindquist.net/generalmicro/102dil3.html). The resistance to various stress conditions was expressed as 'survival rate', which was calculated by dividing the number of stress-treated viable cells by that of nontreated cells (Çakar *et al.*, 2009). In addition, the percent survival rate was calculated according to the following equation;

$$\text{Percent survival rate} = [\text{number of stress-treated viable cells}/\text{number of non-stress-treated viable cells}] \times 100$$

Determination of nickel content

Cultures were inoculated into 10 mL YMM containing 0.15–3.5 mM $NiCl_2$ and grown for 24 h at 30 °C and 150 r.p.m. The cells were collected by centrifugation at 5000 ***g*** for 5 min and washed twice with distilled water, and the supernatants were discarded. The pellets were dried for 12 h at 80 °C and cooled in a dessicator for 20 min, and cell dry weight (CDW) was measured. All samples were then hydrolyzed using 10 M nitric acid. Using a flame atomic absorption spectrometer (Varian AA 280 FS, Australia), the internal concentration of nickel in the samples was determined. Air–acetylene flame was used. The wavelength, slit width, and other experimental parameters were adjusted according to the recommendations given by the manufacturer.

Physiological characterization of the reference strain and the nickel-resistant mutant in the presence and absence of $NiCl_2$

Determination of glucose, ethanol, acetate, and glycerol by HPLC analysis

Precultures of the reference strain and the nickel-resistant mutant were grown overnight in 100 mL YMM at 30 °C and 150 r.p.m. Aliquots of those precultures were inoculated into YMM liquid medium to an initial $OD_{600\ nm}$ of 0.25. Cultivation was performed in 2-L flasks containing 400 mL medium; one control flask with YMM and another

flask supplemented with 0.15 mM $NiCl_2$ were incubated at 30 °C and 150 r.p.m. for 30 h. Cell growth was monitored by regularly measuring $OD_{600\ nm}$ values as triplicates. 1.5-mL samples were taken from each flask at regular intervals and centrifuged at 10 000 ***g*** for 5 min. Supernatants were filtered using a 0.2-μm filter (TPP Techno Plastic Products, Switzerland) and analyzed by high-performance liquid chromatography to determine the ethanol, acetate, and glycerol production as well as glucose consumption rates. The HPLC system was composed of a system controller (Shimadzu SCL – 10A, Japan), liquid chromatography unit (Shimadzu LC-10AD, Japan), degasser (Shimadzu DGU-14A, Japan), refractive index detector (Shimadzu RID-10A, Japan), auto injector (Shimadzu SIL-10AD, Japan), and column oven (Shimadzu CTO-10AC, Japan). HPLC analysis of metabolites was carried out using an Aminex© HPX-87H column at 60 °C with a flow rate of 0.6 mL min^{-1} and 20 μL injections from samples in vials. 5 mM H_2SO_4 solution was used as mobile phase/eluent for HPLC measurements. Six standard solutions of these metabolites were prepared and run one by one to obtain their corresponding standard curve. Concentrations of glucose, ethanol, acetate, and glycerol were calculated by comparison of the data obtained from each sample with the data obtained from six known solutions.

Quantitative assessment of glycogen and trehalose contents via enzymatic assay

The glycogen and trehalose concentrations of the reference strain and the nickel-resistant mutant strain of *S. cerevisiae* were quantitatively assessed in the presence and absence of nickel stress. These intracellular carbohydrates were determined based on a previously described method by Parrou & François, (1997). The method involves amyloglucosidase and trehalase treatment of the samples. The amount of glucose released from trehalose and glycogen was determined by glucose oxidase/peroxidase method (Cramp, 1967). Briefly, suspensions were centrifuged at 5000 ***g*** for 3 min. Twenty microliters of supernatants was added onto 200 μL glucose oxidase/peroxidase reagent (Sigma) in a 96-well plate. The samples were incubated at 37 °C in the dark for 30 min, after which their absorbance at 490 nm was read using a Bio-Rad Benchmark Plus microplate reader (Bio-Rad).

Whole-genome transcriptomic analysis of a nickel-resistant mutant and the reference strain

DNA microarray analysis was performed for the reference strain and the nickel-resistant mutant M9 using Agilent yeast DNA microarray systems. For this purpose, precultures were grown in 20 mL YMM in 100-mL flasks at 30 °C and 150 r.p.m. They were inoculated into 100 mL fresh YMM in 500-mL flasks at an initial $OD_{600\ nm}$ of about 0.1 and incubated at 30 °C and 150 r.p.m. until an $OD_{600\ nm}$ of about 1 (5×10^7 cells mL^{-1}). Each culture was grown as three replicates. RNA was isolated using RNeasy Mini Kit (QIAGEN). Isolated RNA samples were stored at −80 °C.

The RNA content (ng μL^{-1}) of the samples and their RNA integrity numbers (RIN) were determined using a microvolume UV-Vis spectrophotometer (NanoDrop 2000) and Agilent 2100 BioAnalyser, respectively. To determine the RIN values of the RNA samples, the Agilent 6000 Nano Kit was used according to the manufacturer's instructions. RNA samples with RIN values higher than 8 were included in transcriptomic analysis.

The final RNA concentrations of the samples were adjusted to 200 ng μL^{-1}. Agilent One-Color RNA Spike-In Kit was used to provide the internal controls. cRNA samples were labeled with cyanine 3 (Cy3). Cy3-labeled samples were purified using Absolutely RNA Nanoprep Kit (Agilent). They were incubated on microarray slides inside a microarray hybridization chamber (Agilent) in a hybridization oven for 17 h at 65 °C. The microarray slides were scanned upon performing the washing steps according to the manufacturer's instructions. To assess the reliability of the gene expression data, Student's *t*-test was applied along with Benjamini & Hochberg (1995) *P* value correction. Corrected *P* values < 0.05 were considered for significantly different gene expression analysis, and genes with at least twofold change (increase and decrease) in expression and a *P* value less than or equal to 0.01 were chosen for further (cluster) analysis. The DNA microarray experiment was performed in triplicate for all samples, using three independent cultures for each sample. All genes the expression of which changed more than twofold were classified into clusters and functional categories using FUNSPEC online software (Robinson *et al.*, 2002) and FunCat database (http://mips.helmholtz-muenchen.de/proj/funcatDB) (Ruepp *et al.*, 2004).

Determination of expression levels of selected genes by qRT-PCR

Quantitative real-time RT-PCR was performed in the presence and absence of nickel treatment to determine the expression levels of selected genes, which seem to be nickel- or metal-stress-related. Moreover, significantly up- or downregulated genes based on microarray data were verified by qRT-PCR. Reference strain and nickel-resistant mutants were grown in the presence and absence of 0.15 mM $NiCl_2$ until logarithmic phase. Total RNA extraction was performed from these cultures as described

in Section Whole-genome transcriptomic analysis of a nickel-resistant mutant and the reference strain. The RNA content (ng μL^{-1}) of the samples was determined using a microvolume UV-Vis spectrophotometer (NanoDrop 2000). cDNA synthesis was performed using Transcriptor First-Strand cDNA Synthesis kit (Roche), and the initial amount of RNA for each sample was adjusted to 1 μg, according to manufacturer's instructions. The purity and RNA and cDNA concentration of the samples were analyzed by determining OD_{260}/OD_{280} and 260/230 nm absorption ratios, respectively.

The expression levels of the selected genes *AFT1*, *FET3*, *FTR1*, *COT1*, *CCC1*, and *CTT1* were quantified using SYBR Green chemistry (Light Cycler 480 SYBR Green 1 Master Kit, Roche, Cat no: 04 707 516 001). *ACT1* was chosen as the reference gene. All primers were purchased/synthesized from Invitrogen. All amplifications were performed as 20 μL reactions in Light Cycler 480 Equipment (Roche). Cycling conditions were as follows: denaturation for 10 s at 95 °C, followed by 45 cycles of 10 s at 95 °C, 15 s at 56 °C, 20 s at 72 °C, and one cycle of melting for 5 s at 95 °C, 1 min at 65 °C. The reaction was completed with denaturation at 40 °C for 10 s. All reactions were performed in triplicates. Analysis of the qRT-PCR data was performed using the comparative C_T method, also referred as the $2^{-\Delta\Delta C_T}$. In this method, relative gene expression was investigated; the expression level of a gene of interest is considered with respect to that of an internal control gene (Schmittgen & Livak, 2008).

Results

Selection of nickel-resistant mutant populations and individuals by evolutionary engineering

Prior to selection experiments, the MIC for $NiCl_2$ was determined for both reference strain and the EMS-mutagenized starting population for selection. The results showed that cell growth was reduced by 50% in the presence of 0.3 mM or higher $NiCl_2$ concentrations for both reference strain and the EMS-mutagenized population (data not shown). Based on this information, 0.05 mM $NiCl_2$ was chosen as the initial, mild stress level for selection experiments.

As described in Section Evolutionary engineering strategy for selection of nickel-resistant yeast mutants, batch selection began by cultivation in the presence of 0.05 mM $NiCl_2$ as the initial nickel stress level. To estimate the possible inhibitory effect of $NiCl_2$ on the culture, the final $OD_{600\ nm}$ of the first passage was compared with that of the control group grown without $NiCl_2$, and the results showed that this level of $NiCl_2$ had no significant effect on the survival of the first passage. After achieving 2.45 mM $NiCl_2$ concentration within 48 successive passages (about 192 generations), the mean value of percent survival rates was as high as 83% (data not shown). Although this stress level was sufficient to show that the mutant population was capable of growing at high concentrations of $NiCl_2$, the $NiCl_2$ concentration was further increased during successive passages to obtain nickel hyper-resistant mutants in a rapid way. After a selection for 10 further passages, a final mutant population was obtained at the 94th passage (about 376 generations) that could resist 5.3 mM $NiCl_2$. Individual mutant colonies were randomly isolated from that final population, which was plated on solid YMM. The individual mutants were named as M1 to M12.

The next step involved the detailed investigation of nickel resistance of the individual mutants. To this end, all selected individual mutants (M1 to M12) were tested, along with the reference strain and the final population. Nickel resistances were determined upon cultivation at 0.15 and 3.5 mM $NiCl_2$, using MPN assay. After 72 h of incubation, the results showed that although 0.15 mM $NiCl_2$ significantly inhibited the growth of the reference strain, it had a negligible effect on the survival of the mutant individuals (data not shown). Additionally, at 3.5 mM $NiCl_2$, individuals M9, M10, and M12 showed the highest nickel resistances, among all isolated individuals tested (Fig. 1). The reference strain, however, could not grow at all at 3.5 mM $NiCl_2$ concentration. Genetic stability tests were performed for M9, M10, and M12 by analyzing their nickel stress resistance upon ten repetitive batch growth cycles or passages (about 40 generations) under nonselective growth conditions. Among all mutants tested, M9 showed the highest

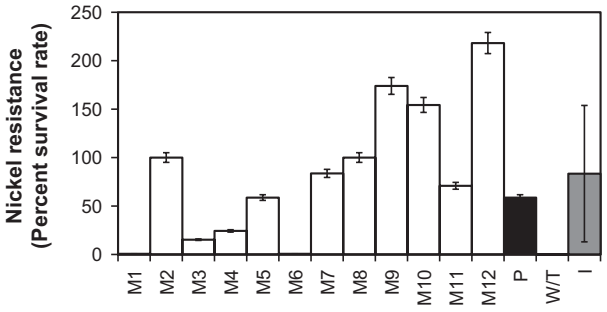

Fig. 1. Nickel resistances (as percent survival rates) of reference strain (W/T) *Saccharomyces cerevisiae*, final mutant population, and 12 mutant individuals isolated from the final mutant population, when grown in the presence of 3.5 mM $NiCl_2$. M1–M12 are mutant individuals, and P and I correspond to the final mutant population and the arithmetic mean resistance values of 12 mutant individuals tested, respectively. The percent survival rates were determined by the MPN method upon incubation at 30 °C for 72 h in the presence of 3.5 mM $NiCl_2$.

genetic stability (data not shown). Analytical polymerase chain reaction (PCR) of the histone promoter genes of M9 (Bell, 2004) confirmed that it is a *S. cerevisiae* strain and not a contaminant. The high level of variation in nickel stress resistances of individual mutants may indicate that nickel resistance has a genetically complex mechanism where multiple genes may play a role as subunits of an intracellular network. In a simple classical genetic analysis, the mutant strain M9 was back-crossed with the strain CEN.PK 113-1A (opposite mating type of the reference strain CEN.PK 113-7D). The resulting heterozygous diploid was more resistant to nickel than the reference strain, but less resistant than M9 (data not shown). This result indicated that nickel resistance was semi-dominant and related to more than one gene.

Phenotypic properties of nickel-resistant *S. cerevisiae* mutants

To test whether nickel-resistant mutants also had cross-resistance against other stress types, twelve individual *S. cerevisiae* mutants (M1 to M12) were grown in the presence of a variety of stress conditions, such as cobalt, iron, manganese, zinc, magnesium, copper, oxidative (hydrogen peroxide), ethanol, salt (NaCl) stress, and BPS (Bathophenanthroline sulfonate, iron chelator; Fig. 2). First, cross-resistance tests were performed on Petri dishes following the routine spotting assay procedure with several dilutions, and for a quantitative estimation of cross-resistances, MPN assay was performed in 96-well plates. Spotting assay results revealed that the mutant with the highest nickel resistance and genetic stability, M9, showed the best cross-resistant phenotype to cobalt, iron, manganese, and zinc. However, it was sensitive to magnesium, copper, hydrogen peroxide, ethanol, salt, and BPS. The other mutant individuals also showed similar behavior (data not shown).

According to spotting assay results, mutants M1, M8, M9, M10, and M11 and the final mutant population (N94) were tested further to quantitatively determine their cross-resistances by MPN assay (Fig. 3). The results showed that all mutants tested had higher resistance than the reference strain against the metals tested. Particularly, the mutant M9 had significantly higher resistance than the other mutants, indicating that the metals tested had no inhibitory effect on that mutant at the applied levels, as it seems to have grown better in the presence of those metals than in control medium. The survival rate of M9 in the presence of cobalt was about 20 000-fold of that of the reference strain. 2.5 mM $CoCl_2$, on the other hand, had a lethal effect on the reference strain. Same results were also observed in the case of iron stress. M9 was also highly resistant to 20 mM $MnCl_2$

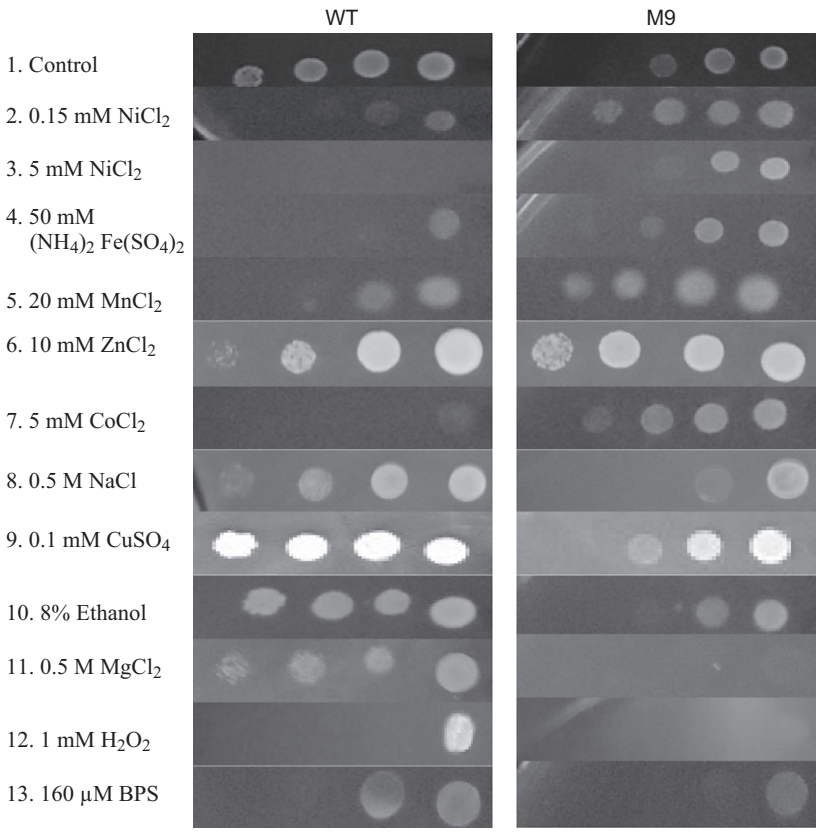

Fig. 2. Cross-resistance test results of reference strain and the nickel-evolved mutant M9 to metal ions and other stress factors. The results are based on serial dilution (from left to right: 10^{-1}–10^{-4}) and growth on solid YMM plates at 30 °C for 72 h in the presence of stress factors.

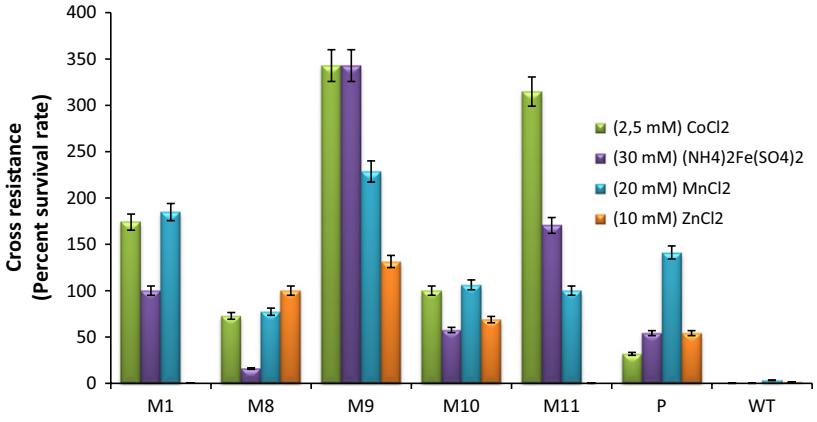

Fig. 3. Cross-resistances of selected mutant individuals (M1–M11), population (P), and the reference strain (WT) to $(NH_4)_2Fe(SO_4)_2$ (30 mM), $CoCl_2$ (2.5 mM), $MnCl_2$ (20 mM), and $ZnCl_2$ (10 mM), as determined by MPN method upon incubation at 30 °C for 72 h.

and 10 mM $ZnCl_2$. It had a higher survival rate than the other mutants and the reference strain. A significantly higher level of manganese resistance was observed in mutant M9 with a survival rate of about 70-fold of that of the reference strain (Fig. 3). On the other hand, M1 and M11 were hypersensitive to zinc stress, and their survival rates were significantly lower than that of the reference strain.

Finally, combined analysis of spotting and MPN assays revealed that among those mutants tested, the nickel hyper-resistant and genetically stable mutant M9 gained cross-resistance against other transition metals such as cobalt, iron, zinc, and manganese, which are in the vicinity of the nickel element in the periodic table of elements. On the contrary, the mutant M9 was unable to grow in other stress conditions where the reference strain *S. cerevisiae* was able to grow. On the basis of these results, the nickel hyper-resistant mutant, M9, with significant cross-resistance against other transition metals was chosen for further detailed physiological and transcriptomic analyses.

Growth physiology of nickel-resistant *S. cerevisiae* mutants

Metabolite consumption and production profile during batch cultivation

During aerobic growth on glucose, the maximum specific growth rate (μ_{max}) and the growth behavior of the nickel-resistant mutant 'M9' were not significantly affected by the presence of 0.15 mM $NiCl_2$. However, the reference strain showed about 40% decrease in maximum specific growth rate, when grown in the presence of 0.15 mM $NiCl_2$ (Fig. 4a). In nickel-free medium, M9 utilized glucose more slowly than the reference strain, due to its slightly extended lag phase and delayed growth. However, glucose consumption rate of M9 was not affected by the presence of 0.15 mM $NiCl_2$, unlike the reference strain that could utilize only about 50% of the initial glucose, most likely due to growth inhibition by nickel (Fig. 4b). In the absence of nickel stress, the reference strain produced the highest amounts of ethanol, glycerol, and acetate (Figs. 4c–e). The production of these metabolites by M9 was not affected by the presence of nickel, however; it was significantly reduced in the case of the reference strain.

Storage carbohydrate production

Trehalose and glycogen have similar functions such as being storage carbohydrates and stress protectants (François & Parrou, 2001). Thus, the intracellular trehalose and glycogen levels of the nickel-tolerant mutant 'M9' and the reference strain culture were determined to find the possible effects of these reserve carbohydrates on nickel resistance (Table 1). The intracellular trehalose levels of M9 in the absence of nickel stress were slightly higher than those of the reference strain, which may provide M9 a survival advantage upon exposure to stress conditions. Additionally, the maximum trehalose concentrations of the reference strain and M9 increased by 3-and 1.5-fold, respectively, in response to nickel stress. This increase could result from nickel-induced oxidative stress, as reported previously (Valko *et al.*, 2005). In the case of glycogen production, M9 produced slightly higher amounts of glycogen, similar to trehalose results. However, exposure to nickel ions did not significantly increase glycogen production in M9.

Determination of nickel contents associated with cells

Nickel accumulation of the reference strain and individual mutant 'M9' were investigated in the presence of 0.15, 1, and 3.5 mM $NiCl_2$ by flame atomic absorption spectrophotometer (Fig. 5). It was found that nickel accumulation profiles of M9 and the reference strain were similar at 0.15 and 1 mM $NiCl_2$ level. However, when

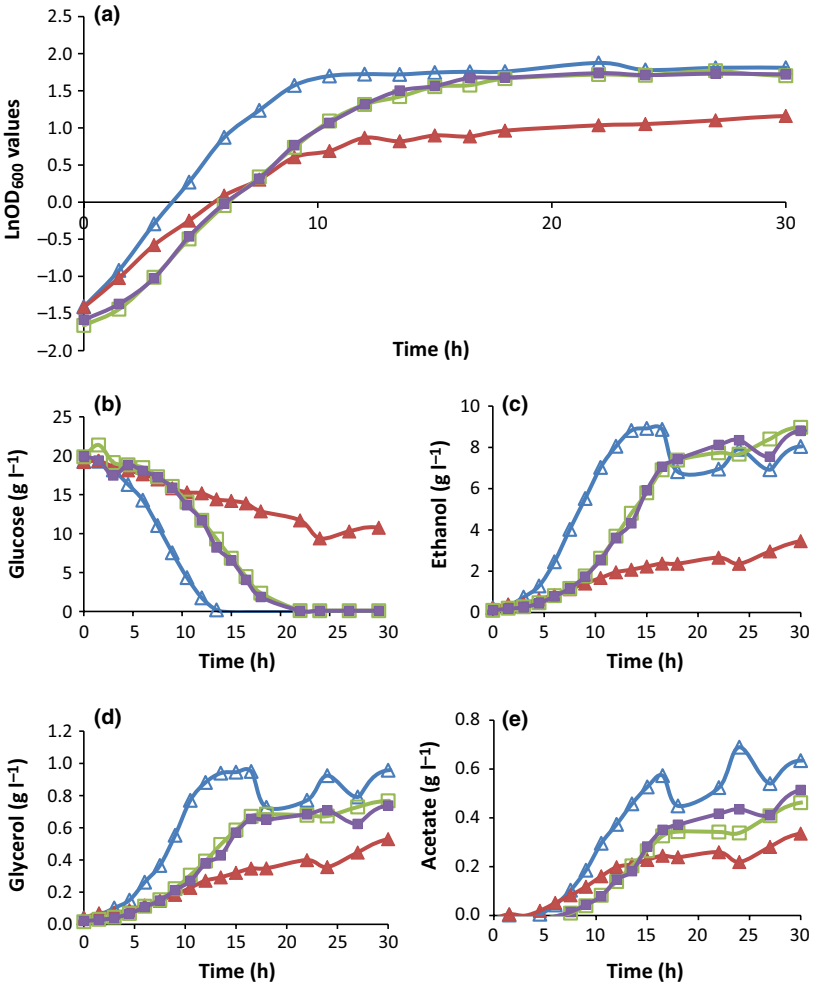

Fig. 4. Growth behavior of reference strain and the nickel-resistant mutant, M9, in minimal medium in the absence or presence of 0.15 mM $NiCl_2$. '▵' Indicates reference strain, '▲' indicates reference strain treated with $NiCl_2$, '□' indicates M9, and '■' indicates M9 treated with $NiCl_2$. (a) Growth curves (Ln $OD_{600\ nm}$ vs. time). (b) Residual glucose concentrations. (c) Ethanol, (d) glycerol, and (e) acetate concentrations vs. time.

Table 1. Intracellular trehalose and glycogen contents (mg glucose equivalents mg^{-1} CDW) of WT and the nickel-resistant mutant M9 grown in YMM in the absence and presence of 0.15 mM $NiCl_2$

Time (h)	WT	WT-Ni	M9	M9-Ni
Trehalose content per cell dry weight (mg glucose equivalents mg^{-1} CDW)				
7.5	0.017	0.032	0.037	0.033
10	0.016	0.031	0.041	0.048
14	0.030	0.035	0.060	0.081
22	0.017	0.077	0.048	0.045
30	0.013	0.089	0.031	0.032
Glycogen content per cell dry weight (mg glucose equivalents mg^{-1} CDW)				
7.5	0.021	0.034	0.032	0.033
10	0.016	0.026	0.041	0.033
14	0.043	0.028	0.075	0.088
22	0.017	0.033	0.043	0.032
30	0.014	0.027	0.031	0.028

$NiCl_2$ concentration was increased to 3.5 mM, nickel accumulation increased about twofold in M9, while no increase was observed in reference strain cells. This result combined with the lethal effect of higher $NiCl_2$ concentrations on the reference strain cells may suggest that nickel accumulation of the reference strain cells at higher $NiCl_2$ levels was probably caused by the sorption of the dead cells. Additionally, nickel-resistant *S. cerevisiae* cells with high nickel content imply that these cells might have avoided the toxic effect of nickel by sequestering it inside the cell, probably in the vacuole, rather than pumping it out of the cell by an efflux system.

Whole-genome transcriptomic analysis of nickel-resistant mutant

Whole-genome transcriptomic analyses of the nickel-resistant mutant M9 and the reference strain were performed to gain insight into the genetic mechanisms of nickel resistance in *S. cerevisiae*. Statistical analysis revealed that 640 genes were upregulated, and 369 genes were downregulated. Classification of those genes into clusters and functional categories by FUNSPEC online software and FUNCAT database revealed the following results: the genes

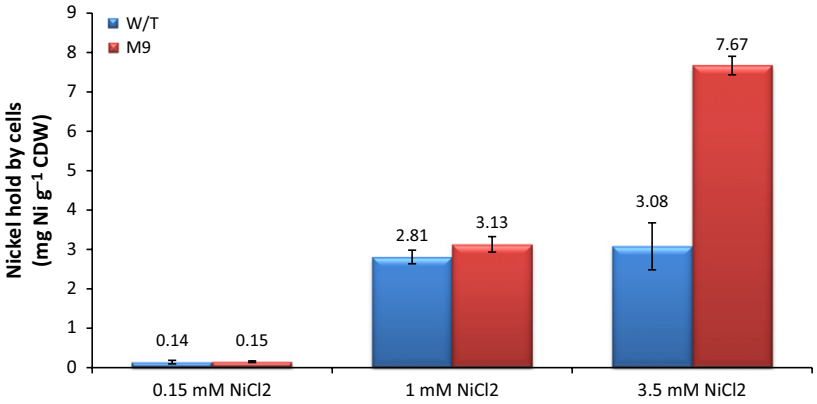

Fig. 5. Nickel contents (per CDW) of the reference strain and mutant individual M9, as determined by FAAS upon 24-h cultivation under 0.15–3.5 mM $NiCl_2$ stress conditions. All experiments were performed in triplicates.

related to iron homeostasis, stress response, and oxidative damage were significantly induced. Additionally, metal homeostasis, protein refolding, and trehalose and glycogen metabolism genes were also upregulated. On the other hand, majority of the downregulated genes were related to ribosome biogenesis, translation, rRNA processing, and methylation (Tables 2 & 3 and Fig. 6). Iron metabolism genes were also upregulated in the present study.

In *S. cerevisiae*, iron homeostasis is highly regulated by the two transcription factors, Aft1 and Aft2, and the genes regulated by these two transcription factors are referred to as the iron regulon (Yamaguchi-Iwai *et al.*, 1995; Blaisseau *et al.*, 2001). Aft1p binds to a conserved promoter sequence and activates the expression of target genes in response to iron starvation. In iron-depleted conditions, Aft1 translocates from cytoplasm to nucleus and vice versa. Aft2 also regulates the expression of iron regulon, but with a weaker transcriptional activity (Rutherford *et al.*, 2005). In this study, among the 21 iron metabolism genes whose expression changed more than twofold compared with the reference strain, 16 of them are regulated by Aft1. *AFT2* was also upregulated, but not as much as *AFT1*. Arita *et al.* (2009) reported that deletion of *AFT1* gene in *S. cerevisiae* resulted in decreased resistance to nickel sulfate. It is known that nickel ions chemically and structurally resemble to metal ions such as zinc, cobalt, and iron and displace these metal ions from the cell. Additionally, nickel compounds interfere with iron uptake, possibly resulting in iron depletion and thus overexpression of iron homeostasis-related genes. It was also reported that exposure to nickel reduces intracellular iron levels in plant and animal cells (Ruotolo *et al.*, 2008).

Among the Aft1p-regulated genes, expression of *TIS11*/*CTH2* was about 50 times higher than that of the reference strain. In response to iron deficiency, Tis11p degrades the mRNAs of the proteins involved in Fe-dependent processes. The function of Tis11p is binding to specific AU-rich elements in the 3′ untranslated region of those mRNAs, which results in degradation of mRNA molecules. It was stated that the role of *TIS11* is significantly important in iron-limited conditions, and expression of *TIS11* in *aft1Δ* mutants was greatly decreased (Puig *et al.*, 2005).

Expression level determination by quantitative RT-PCR

Quantitative RT-PCR was performed to confirm the upregulation of *AFT1*, *FET3*, *FTR1*, *CCC1*, *COT1*, and *CTT1*. In our previous work, we had obtained cobalt hyper-resistant *S. cerevisiae* mutants that were also cross-resistant to nickel stress (Çakar *et al.*, 2009). Thus, similarities were expected between resistance mechanisms to nickel and cobalt stress. Transcriptomic analysis of our evolved cobalt hyper-resistant mutant revealed that the iron regulon was constitutively activated (Alkim *et al.*, 2013), which largely depends on the transcriptional activator Aft1 (Yamaguchi-Iwai *et al.*, 1995). *AFT1* was upregulated by 2.01-fold (Alkim *et al.*, 2013). The other upregulated genes of the iron homeostasis cluster included *FET3* and *FTR1*, which encode proteins involved in high-affinity iron uptake (De Silva *et al.*, 1995). The product of these genes increases cytosolic iron content (Philpott & Protchenko, 2008) whenever it is not sufficient. *FET3* was upregulated by 18.33-fold, and *FTR1*, by 4.67-fold (Alkim *et al.*, 2013) in the cobalt hyper-resistant mutant. *COT1* encodes a vacuolar membrane protein for cobalt and zinc transport from the cytosol to the vacuole (Stadler & Schweyen, 2002), and the expression of this cobalt-related gene was also increased by twofold in the cobalt hyper-resistant mutant. *CTT1* that encodes catalase T and *CCC1* encoding a vacuolar iron transporter (Li *et al.*, 2001) were strongly repressed in the cobalt hyper-resistant mutant. To test whether there are also similar

Table 2. Upregulated genes (about twofold and higher) in M9, in comparison with WT yeast, based on microarray analysis

ORF name	Gene name	Fold change	ORF name	Gene name	Fold change
Iron metabolism			Cellular response to oxidative stress		
YGL071W	*AFT1*	1.48	YMR250W	*GAD1*	6.34
YMR058W	*FET3*	8.71	YBL064C	*PRX1*	3.41
YER145C	*FTR1*	2.86	YCL035C	*GRX1*	2.46
YLR136C	*TIS11/CTH2*	51.39	YHR104W	*GRE3*	3.33
YOR382W	*FIT2*	34.21	YKL026C	*GPX1*	2.46
YOR383C	*FIT3*	21.45	YKL086W	*SRX1*	2.32
YLR214W	*FRE1*	4.57	YLR220W	*CTT1*	1.95
YKL220C	*FRE2*	2.65	Trehalose metabolism		
YOR381W	*FRE3*	3.52	YML100W	*TSL1*	14.80
YNR060W	*FRE4*	3.54	YBR126C	*TPS1*	2.84
YLL051C	*FRE6*	5.68	YDR074W	*TPS2*	4.35
YLR047C	*FRE8*	2.43	YDR001C	*NTH1*	2.53
YHL040C	*ARN1*	6.92	Glycogen biosynthetic process		
YEL065W	*ARN3/SIT1*	13.30	YEL011W	*GLC3*	8.28
YOL158C	*ARN4/ENB1*	10.96	YFR017C	*IGD1*	7.12
YLR220W	*CCC1*	1.63	YFR015C	*GSY1*	6.19
YDR270W	*CCC2*	4.35			
YLL029W	*FRA1*	7.48	Amino acid metabolism		
YBR295W	*PCA1*	2.35	YPL265W	*DIP5*	30.59
YLR034C	*SMF3*	5.03	YDR046C	*BAP3*	17.68
YPL135W	*ISU1*	2.29	YCL025C	*AGP1*	8.63
Stress response			YHR137W	*ARO9*	5.99
YPR160W	*GPH1*	11.47	YLL055W	*YCT1*	6.39
YIL101C	*XBP1*	7.91	YGL184C	*STR3*	2.60
YBR072W	*HSP26*	8.07	YGR142W	*BTN2*	7.62
YPL280W	*HSP32*	3.95	Glucose metabolism		
YGR154C	*GTO1*	4.10	YFR053C	*HXK1*	33.18
YNR034W-A		5.94	YHR096C	*HXT5*	12.56
YLL039C	*UBI4*	11.05	YDR343C	*HXT6*	14.40
YLL026W	*HSP104*	9.30	YDR342C	*HXT7*	16.33
YDR258C	*HSP78*	7.71	YMR105C	*PGM2*	15.95
Metal homeostasis			Glutathione metabolic process		
YLR411W	*CTR3*	4.87	YGR154C	*GTO1*	4.09
YOR316C	*COT1*	2.39	YKR076W	*ECM4*	5.17
YLL009C	*COX17*	2.52	YLL060C	*GTT2*	4.78
Protein refolding			YMR251W	*GTO3*	7.75
YPL240C	*HSP82*	6.82	Functionally unknown genes		
YDR258C	*HSP78*	7.71	YMR095C	*SNO1*	74.98
			YNL194C		15.21

expression level changes in those iron-related genes of the nickel hyper-resistant mutant, the expression levels of the above-mentioned genes were determined also for the nickel hyper-resistant mutant M9. For this purpose, cultures of the reference strain and M9 were incubated in both the absence and presence of 0.15 mM $NiCl_2$.

Aft1p is the transcription regulator, which controls nearly 25 genes on the iron regulon (Philpott & Protchenko, 2008). DNA microarray analysis results demonstrated that iron regulon was activated in M9 compared with reference strain, and *AFT1* was 1.48-fold upregulated in M9 compared with the reference strain (Table 2). This upregulation might explain the increase in the expression level of the iron homeostasis genes. The upregulation of *AFT1* in M9 was verified by qRT-PCR, and it was again found to be upregulated in M9 with a fold change of 2.13 compared with the reference strain (Table 4). Nickel treatment also caused upregulation of reference strain *AFT1* by 1.86-fold compared with the untreated cells of reference strain. It was observed that *AFT1* upregulation did not change significantly for the nickel-treated and untreated cultures of M9, showing that M9 has high levels of *AFT1* expression already in the absence of any nickel stress.

FET3 encodes one of the most important proteins for high-affinity iron uptake system (Askwith *et al.*, 1994). Thus, its expression was also tested via qRT-PCR. A positive correlation was also observed between microarray and qRT-PCR data also for *FET3* gene in M9. It was

Table 3. Downregulated genes (about twofold and higher) in M9, as compared to WT yeast, based on microarray analysis

ORF name	Gene name	Fold change	ORF name	Gene name	Fold change
Nucleobase transport			Pheromone regulated genes		
YER060W	*FCY21*	14.33	YDL039C	*PRM7*	5.12
YER060W-A	*FCY22*	6.22	Methyltransferase activity		
Metal homeostasis			YNL024C		4.99
YML123C	*PHO84*	13.27	YBR034C	*HMT1*	4.12
YMR319C	*FET4*	4.20	YBR061C	*TRM7*	2.23
YMR243C	*ZRC1*	1.71	Translation		
Ribosome biogenesis			YAL025C	*MAK16*	3.59
YGR159C	*NSR1*	6.15	YBR079C	*RPG1*	2.14
YNL002C	*RLP7*	2.21	YCL037C	*SRO0*	2.55
YJL122W	*ALB1*	5.61	YDL081C	*RPP1A*	2.17
YDR101C	*ARX1*	4.70	YDR091C	*RLI1*	2.20
YCR072C	*RSA4*	4.39	YHR021C	*RPS27B*	2.10
YHL033C	*RPL8A*	5.86	rRNA processing		
YKL006W	*RPL14A*	2.14	YDR083W	*RRP8*	4.52
YBR191W	*RPL21A*	2.09	YDL060W	*TRS1*	4.01
YBR267W	*REI1*	4.05	YOL077C	*BRX1*	2.84
Peptide transporter			Amino acid transport		
YPR194C	*OPT2*	6.07	YBR069C	*TAT1*	4.48
Helicase activity			YNL065W	*AQR1*	3.02
YKL078W	*DHR2*	5.83	Glyoxylate cycle		
YNL112W	*DBP2*	5.69	YBR084W	*MLS1*	2.16
YJL033W	*HCR4*	4.00	YIR031C	*DAL7*	4.20
Kinase activity			Post-transcriptional regulation		
YNR012W	*URK1*	2.57	YOR359W	*VTS1*	4.16

observed that *FET3* was highly expressed in M9, about fourfold of the reference strain. High expression of *FET3* could explain the high iron resistance of individual mutants, independent from nickel resistance. Interestingly, *FET3* expression level of M9 decreased upon nickel treatment. It was also found that expression of *FET3* was downregulated in nickel-treated reference strain cells.

High-affinity iron uptake is mediated by not only Fet3p but also Ftr1p, which is a plasma membrane permease (Stearman *et al.*, 1996). According to the qRT-PCR results, *FTR1* was 3.50-fold upregulated in M9 with respect to the reference strain under control conditions, consistent with microarray results (Table 2 and 4). However, unlike *FET3, FTR1* expression upon nickel treatment increased in both reference strain and M9, when compared to their corresponding control group.

According to cross-resistance results (Figs 2 and 3), it was thought that resistance to nickel and cobalt could share common mechanisms because cross-resistance phenotype of the nickel-resistant mutants to many stress conditions tested was similar to that of a cobalt-resistant mutant (Çakar *et al.*, 2009). Therefore, expression levels of *COT1* involved in cobalt detoxification were also determined, along with the genes related to vacuolar metal uptake (*CCC1*) and general stress response (*CTT1*) under control and stress (nickel) conditions.

Cot1p compartmentalizes cobalt and zinc ions into the vacuole, and overexpression of *COT1* confers resistance to these ions in reference strain cells (Conklin *et al.*, *1994*). Normalized fold expression values showed that treated and untreated M9 cells expressed *COT1* about twofold higher than the reference strain, and *COT1* expression in reference strain cells was also upregulated when cells were exposed to $NiCl_2$ (Table 4). Considering the sequestration of nickel ions into the vacuole in stress conditions and the putative cobalt–nickel relationship, this result is not surprising. Similar expression patterns were also observed in the case of *CCC1*, which is responsible for iron transport from cytosol to vacuole and vice versa (Li *et al.*, 2001). DNA microarray analysis results also showed that the expression of these vacuolar metal transport genes was upregulated in untreated M9 cells (Table 2). However, unlike cobalt hyper-resistant mutant, both *CCC1* and *CTT1* were upregulated in M9. *S. cerevisiae CTT1*, the gene encoding cytoplasmic catalase T, mediates the decomposition of hydrogen peroxide to oxygen and water and protects the cells from oxidative damage (Bissinger *et al.*, 1989). M9 expressed *CTT1* about 15-fold of the reference strain, even in the absence of nickel stress, and about eightfold of the reference strain in nickel-containing medium (Table 4). Expression data for *CTT1* in microarray experiments also showed that *CTT1* was overexpressed (Table 2). This can be explained by the nickel-induced oxidative damage and formation of reactive oxygen

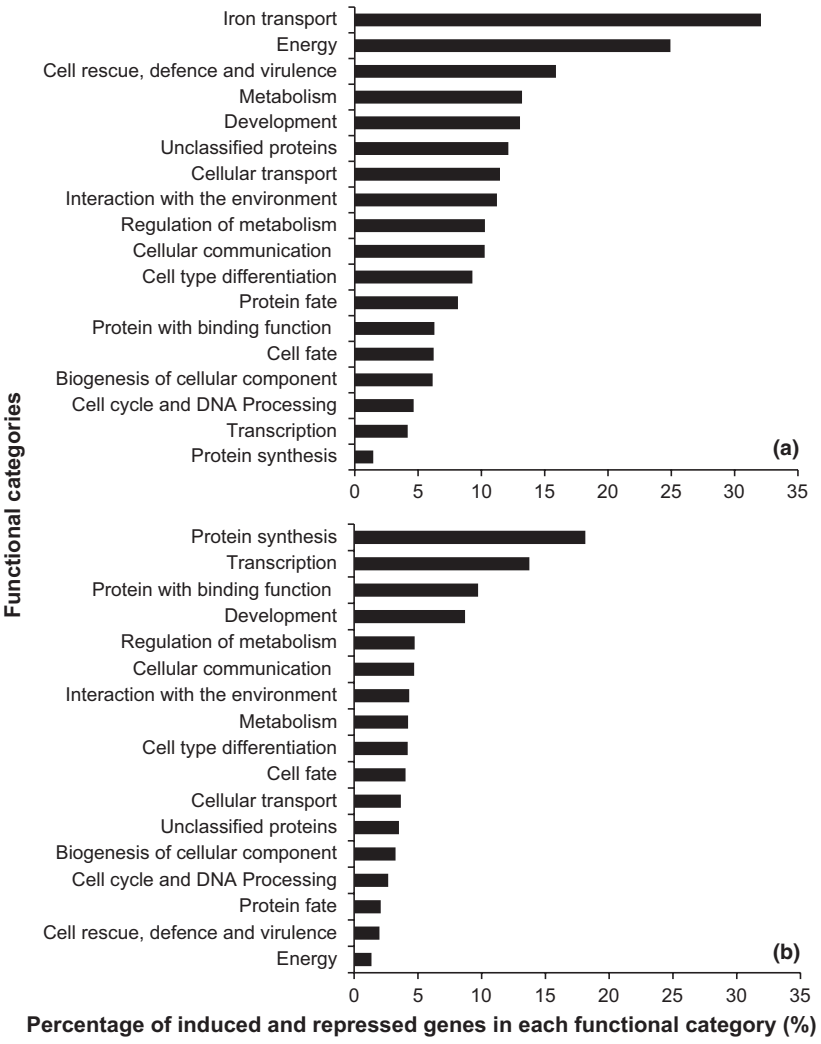

Fig. 6. Functional categories of induced (a) and repressed (b) ORFs (prepared according to Yasokawa & Iwahashi, 2010).

Table 4. Normalized expression levels of some potentially nickel-related genes in WT and the nickel-resistant mutant M9 in the absence and presence of nickel stress, based on qRT-PCR results

	Expression levels of potentially nickel-related genes (normalized to expression levels of wild type (WT) without nickel stress)					
Strains	*AFT1*	*FET3*	*FTR1*	*COT1*	*CCC1*	*CTT1*
WT-Ni	1.86 ± 0.40	0.84 ± 0.05	2.36 ± 0.15	1.56 ± 0.05	1.47 ± 0.08	3.87 ± 0.13
M9	2.13 ± 0.20	4.33 ± 1.20	3.5 ± 0.20	2.32 ± 0.09	1.96 ± 0.02	14.76 ± 0.56
M9-Ni	2.18 ± 0.13	2.68 ± 0.18	4.16 ± 0.18	2.16 ± 0.07	2.35 ± 0.32	7.59 ± 0.36

species (ROS) via Fenton reaction. Despite *CTT1* upregulation, it is surprising to observe that M9 was hypersensitive to oxidative damage, based on cross-resistance test results (Fig. 2). The fact that the *CTT1* expression in wild type (WT) increased about fourfold upon nickel exposure seems to support the role of cytoplasmic catalase in nickel stress. Thus, molecular factors other than *CTT1* might have been affected in M9, which might have resulted in oxidative damage sensitivity in this mutant.

Discussion

In this study, it was shown that evolutionary engineering is a powerful strategy to obtain nickel hyper-resistant *S. cerevisiae* mutants. This is the first report on the physiological and transcriptomic analysis of a nickel hyper-resistant *S. cerevisiae* strain that has been successfully obtained by evolutionary engineering. The results of the physiological and transcriptomic analyses of a nickel hyper-resistant

S. cerevisiae mutant were compared with the results of previous studies with metal-sensitive deletion mutants and/or nickel-exposed reference strains of *S. cerevisiae*, as well as with a cobalt hyper-resistant *S. cerevisiae* mutant obtained by our group (Çakar *et al.*, 2009; Alkim *et al.*, 2013).

Takumi *et al.* (2010) investigated transcriptomic responses of a reference laboratory strain of *S. cerevisiae* (S288C) to $NiCl_2$ using yeast DNA microarrays. Exposure of *S. cerevisiae* cells grown in YPD medium to a pulse stress of 25 mM $NiCl_2$ followed by DNA microarray analysis revealed that genes related to sulfur amino acid metabolism, iron metabolism, and heavy metal homeostasis were significantly upregulated. Additionally, genes related to oxidative stress response, that is, glutathione peroxidase, thioredoxin and glutaredoxin, and DNA repair were induced. Transcriptomic data were similar to those obtained previously where cobalt stress was shown to induce iron accumulation in yeast cells (Stadler & Schweyen, 2002). Thus, it was suggested that cellular iron is increased by the transcriptional response to nickel stress and also cobalt stress. However, unlike our study, the metal contents were not determined in that study. In the present study on nickel hyper-resistant mutant M9, however, only 4 (*GTT2*, *MHT1*, *STR2*, and *STR3*) of 26 upregulated genes related to sulfur amino acid metabolism in nickel-exposed S288C (Takumi *et al.*, 2010) were found to be also upregulated in M9, and the level of upregulation of those genes in M9 was significantly lower than in S288C. Additionally, genes related to DNA repair were also not upregulated in M9. Besides, stress response genes, genes related to protein refolding; trehalose, glucose, and amino acid metabolism; and glycogen biosynthesis, were upregulated in M9, but they were not found to be upregulated in the reference strain of Takumi *et al.* (2010) upon nickel exposure. The upregulated gene groups that are common to both M9 and the reference strain in Takumi's work are those related to iron metabolism, metal homeostasis, cellular response to oxidative stress, and xenobiotics resistance (*GTT1* and *GTT2*) (Table 2, and Takumi *et al.*, 2010). Although data for downregulated genes were not shown in Takumi *et al.* (2010), it was mentioned that the strongly downregulated genes were related to cell rescue, defense, virulence, subcellular localization metabolism, cellular transport, and protein synthesis. Detailed analysis of both up- and downregulated genes in M9, however, revealed that the genes related to cell rescue, defense, virulence, subcellular localization, metabolism, and cellular transport were upregulated, unlike the reference strain in Takumi *et al.* (2010). Similar to the reference strain in Takumi *et al.* (2010), protein synthesis genes were downregulated in M9, as well as genes related to transcription. It is important to note that the work by Takumi *et al.* (2010) includes transcriptomic analysis of a nickel-exposed laboratory strain of *S. cerevisiae*, which does not have an improved nickel tolerance, unlike the mutant M9 in our study, which is nickel hyper-resistant, and the transcriptomic analysis of which was carried out in the absence of nickel. Thus, differences were expected between the two transcriptomic data, which may provide information on the genetic changes related to nickel tolerance. Additionally, there are more comprehensive data on the growth physiology of the reference strain and the nickel-resistant mutant M9 in the present study, where in Takumi *et al.* (2010), only viability data upon $NiCl_2$ exposure were provided.

Jin *et al.* (2008) investigated the global transcriptome and deletome profiles of *S. cerevisiae* exposed to a variety of transition metals such as copper, silver, zinc, cadmium, mercury, chromium, and arsenic. Transcriptome analysis results revealed common metal response (CMR) genes the expression of which was affected by all metals. CMR genes were found to be associated with a variety of biological processes such as metal ion (particularly iron) transport and homeostasis, detoxification of ROS, carbohydrate and fatty acid metabolism, polyamine transport, and RNA polymerase II transcription. As Aft1- and Aft2-regulated genes (*ARN1*, *ARN2*, *SIT1*, *FTR1*, and *FET3*) which are normally activated when there is iron limitation, were also upregulated upon metal exposure, it was suggested that exposure to high levels of one metal may disrupt the metal-sensing systems of other metals (Jin *et al.*, 2008). The expression levels of genes involved in the biological processes of sulfur metabolism also changed. As in the article by Takumi *et al.* (2010), changes in sulfur amino acid transport and biosynthesis were identified by both transcriptome and deletome analyses. It was also mentioned that this result was consistent with a previous study of arsenic exposure where glutathione synthesis-related processes were found in both transcriptome and deletome (Haugen *et al.*, 2004). Jin *et al.* (2008) concluded that unlike transcriptome analysis results, the deletome analysis results revealed that the resistance to metal toxicity involves metal specific responses. Our transcriptomic analysis results also supported the presence of CMR genes.

Ruotolo *et al.* (2008) studied the genomewide expression of yeast deletion mutant strains exposed to cadmium and nickel. In that study, deletion of iron homeostasis genes, *AFT1*, *FET3*, *FTR1*, *SMF1*, *SMF3,* and *CCC2* caused nickel sensitivity, and those genes were also upregulated in our study (Table 2). Effect of *AFT1* on nickel resistance was also reported by Arita *et al.* (2009). It was also reported that overexpression of *AFT1* confers resistance to nickel ions; however, expression of iron regulon genes was not induced by nickel, according to a previous study (Stadler & Schweyen, 2002). These results suggest

that Aft1p may have direct or indirect effects on nickel resistance mechanism of *S. cerevisiae*. Additionally, sensitivity of M9 to iron depletion (BPS sensitivity) and better growth in iron-supplemented medium could be explained by this highly upregulated iron regulon in M9 mutant (Fig. 2).

Bleackley *et al.* (2011) used high-density arrays to screen a *S. cerevisiae* deletion set that contained gene deletions for strains sensitive to Fe, Cu, Mn, Ni, Zn, and Co. They observed a significant overlap between the strains sensitive to Mn, Zn, Ni, and Co. Many of these strains were lacking genes for the high-affinity Fe transport pathway, vacuolar transport, and acidification. They stated that the components of the high-affinity Fe transport pathway contribute to the tolerance of Cu, Mn, Ni, Co, and Zn. Our results with a nickel hyper-resistant mutant also confirmed the importance of the high-affinity Fe transport pathway.

In our nickel hyper-resistant mutant, sensitivity to $MgCl_2$ (0.5 M), H_2O_2 (1.0 mM), ethanol (8%, 'v/v'), NaCl (0.5 mM), and BPS (160 μM) was observed. Similarly, the cobalt hyper-resistant mutant obtained in our previous study was cross-resistant to $NiCl_2$, but sensitive to $MgCl_2$ (Çakar *et al.*, 2009). Joho *et al.* (1991) reported that a mutant *S. cerevisiae* strain with reduced Mg^{2+} accumulation had higher tolerance to Co^{2+} and Ni^{2+}. Increasing concentrations of Mg^{2+} in the medium reduced the inhibitory effects of Ni^{2+} and Co^{2+}. Thus, they suggested that a reduction in the Co^{2+} and Ni^{2+} uptake by an Mg^{2+} transport system might be a resistance mechanism of that mutant strain. In a later study, Nishimura *et al.* (1998) also reported that Ni^{2+} uptake by *S. cerevisiae* was preferentially inhibited by Mg^{2+}, and nickel toxicity was rescued by the supply of 10 mM $MgCl_2$. Apparently, while evolving for nickel resistance, the nickel hyper-resistant mutant might have undergone cellular changes that might be related to magnesium ion transport. These changes may have resulted in increased sensitivity to high levels of magnesium ions (0.5 M $MgCl_2$). Further studies would be necessary to understand the nature of this apparent 'trade-off' situation in evolutionary engineering (Çakar *et al.*, 2012).

For a detailed genetic characterization of nickel resistance in *S. cerevisiae*, future studies are in progress including resequencing of the evolved strain, as well as preparation and in-depth physiological and genetic analyses of deletion mutants for those highly overexpressed genes in M9, such as *SNO1*, *TIS11*, *TMA10*, *SNZ1*, and *FIT2*.

Acknowledgements

This study was supported by COST Action CM0902 and the Scientific and Technological Research Council of Turkey, TUBITAK (project no: 109T638, PI: Z.P.Ç.). We thank Melike Özgül and Levent Üge for technical assistance and Vernessa Henderson for English proofreading. The authors state that they have no conflict of interests.

References

Alkim C, Benbadis L, Yilmaz U, Cakar ZP & Francois JM (2013) Mechanisms other than activation of the iron regulon account for the hyper-resistance to cobalt of a *Saccharomyces cerevisiae* strain obtained by evolutionary engineering. *Metallomics* **5**: 1043–1060. DOI: 10.1039/C3MT00107E.

Arita A, Zhou X, Ellen TP *et al.* (2009) A genome-wide deletion mutant screen identifies pathways affected by nickel sulfate in *Saccharomyces cerevisiae*. *BMC Genomics* **10**: 524.

Askwith C, Eide D, Van Ho A, Bernard PS, Li L, Davis-Kaplan S, Sipe DM & Kaplan J (1994) The *FET3* gene of *S. cerevisiae* encodes a multicopper oxidase required for ferrous iron uptake. *Cell* **76**: 403–410.

Bell PJL (2004) Yeast differentiation using histone promoter sequences. *Lett Appl Microbiol* **38**: 388–392.

Benjamini Y & Hochberg Y (1995) Controlling the false discovery rate: a practical and powerful approach to multiple testing. *J R Stat Soc Series B Stat Methodol* **57**: 289–300.

Bissinger PH, Wieser R, Hamilton B & Ruis H (1989) Control of *Saccharomyces cerevisiae* catalase T gene (*CTT1*) expression by nutrient supply via the RAS-cyclic AMP pathway. *Mol Cell Biol* **9**: 1309–1315.

Blaisseau PL, Lesuisse E & Camadro JM (2001) Aft2p, a novel iron-regulated transcription activator that modulates, with Aft1p, intracellular iron use and resistance to oxidative stress in yeast. *J Biol Chem* **276**: 34221–34226.

Bleackley MR, Young BP, Loewen CJR & MacGillivray RTA (2011) High density array screening to identify the genetic requirements for transition metal tolerance in *Saccharomyces cerevisiae*. *Metallomics* **3**: 195–205.

Butler PR, Brown M & Oliver SG (1996) Improvement of antibiotic titers from *Streptomyces* bacteria by interactive continuous selection. *Biotechnol Bioeng* **49**: 185–196.

Çakar ZP, Seker UO, Tamerler C, Sonderegger M & Sauer U (2005) Evolutionary engineering of multiple-stress resistant *Saccharomyces cerevisiae*. *FEMS Yeast Res* **5**: 569–578.

Çakar ZP, Alkim C, Turanli B, Tokman N, Akman S, Sarikaya M, Tamerler C, Benbadis L & Francois JM (2009) Isolation of cobalt hyper-resistant mutants of *Saccharomyces cerevisiae* by *in vivo* evolutionary engineering approach. *J Biotechnol* **143**: 130–138.

Çakar ZP, Turanlı-Yıldız B, Alkım C & Yılmaz Ü (2012) Evolutionary engineering of *Saccharomyces cerevisiae* for improved industrially important properties. *FEMS Yeast Res* **12**: 171–182.

Cempel M & Nikel G (2006) Nickel: a review of its sources and environmental toxicology. *Pol J Environ Stud* **15**: 375–382.

Conklin DS, Culbertson MR & Kung C (1994) Interactions between gene products involved in divalent cation transport in *Saccharomyces cerevisiae*. *Mol Gen Genet* **244**: 303–311.

Cramp DG (1967) New automated method for measuring glucose by glucose oxidase. *J Clin Pathol* **20**: 910–912.

De Silva DM, Askwith CC, Eide D & Kaplan J (1995) The FET3 gene product required for high affinity iron transport in yeast is a cell surface ferroxidase. *J Biol Chem* **270**: 1098–1101.

Denkhaus E & Salnikow K (2002) Nickel essentiality toxicity and carcinogenicity. *Crit Rev Oncol Hematol* **42**: 35–56.

Eide DJ, Clark S, Nair TM, Gehl M, Gribskov M, Guerinot ML & Harper JF (2005) Characterization of the yeast ionome: a genome-wide analysis of nutrient mineral and trace element homeostasis in *Saccharomyces cerevisiae*. *Genome Biol* **6**: R77.

Eitinger T & Mandrand-Berthelot MA (2000) Nickel transport systems in microorganisms. *Arch Microbiol* **173**: 1–9.

Eitinger T, Degen O, Bohnke U & Muller M (2000) Nic1p a relative of bacterial transition metal permeases in *Schizosaccharomyces pombe* provides nickel ion for urease biosynthesis. *J Biol Chem* **275**: 33184.

Entian KD & Kötter P (2007) Yeast genetic strain and plasmid collections. *Methods Microbiol* **36**: 629–666.

Farcasanu IC, Mizunuma M, Nishiyama F & Miyakawa T (2005) Role of L-histidine in conferring tolerance to Ni^{+2} in *Saccharomyces cerevisiae* cells. *Biosci Biotechnol Biochem* **69**: 2343–2348.

François J & Parrou JL (2001) Reserve carbohydrates metabolism in the yeast *Saccharomyces cerevisiae*. *FEMS Microbiol Rev* **25**: 125–145.

Guimaraes PM, Francois J, Parrou JL, Teixeira JA & Domingues L (2008) Adaptive evolution of a lactose-consuming *Saccharomyces cerevisiae* recombinant. *Appl Environ Microbiol* **74**: 1748–1756.

Haugen AC, Kelley R, Collins JB, Tucker CJ, Deng C, Afshari CA, Brown JM, Ideker T & Van Houten B (2004) Integrating phenotypic and expression profiles to map arsenic-response networks. *Genome Biol* **5**: R95.

Jin YH, Dunlap PE, McBride SJ, Al-Refai H, Bushel PR & Freedman JH (2008) Global transcriptome and deletome profiles of yeast exposed to transition metals. *PLoS Genet* **4**: e1000053, DOI:10.1371/journal.pgen.1000053.

Joho M, Tarumi K, Inouhe M, Tohoyama H & Murayama T (1991) Co^{+2} and Ni^{+2} resistance in *Saccharomyces cerevisiae* associated with a reduction in the accumulation of Mg^{+2}. *Microbios* **67**: 177–186.

Joho M, Ishikawa Y, Kunikane M, Inouhe M, Tohoyama H & Murayama T (1992) The subcellular distribution of nickel ion in Ni-sensitive and Ni-resistant strains of *Saccharomyces cerevisiae*. *Microbios* **71**: 149–159.

Joho M, Inouhe M, Tohoyama H & Murayama T (1995) Nickel ion resistance mechanisms in yeasts and other fungi. *J Ind Microbiol* **14**: 164–168.

Kasprzak KS, Sunderman FW Jr & Salnikow K (2003) Nickel carcinogenesis. *Mutat Res* **533**: 67–97.

Lawrence CW (1991) Classical mutagenesis techniques. *Methods Enzymol* **194**: 456–464.

Li L, Chen OS, McVey Ward D & Kaplan J (2001) CCC1 is a transporter that mediates vacuolar iron storage in yeast. *J Biol Chem* **276**: 29515–29519.

Minty JJ, Lesnefsky AA, Lin F *et al.* (2011) Evolution combined with genomic study elucidates genetic bases of isobutanol tolerance in *Escherichia coli*. *Microb Cell Fact* **10**: 18.

Mulrooney SB & Hausinger RP (2003) Nickel uptake and utilization by microorganisms. *FEMS Microbiol Rev* **27**: 239–261.

Nevoigt E (2008) Progress in metabolic engineering of *Saccharomyces cerevisiae*. *Microbiol Mol Biol Rev* **72**: 379–412.

Nishimura K, Igarashi K & Kakinuma Y (1998) Proton gradient-driven nickel uptake by vacuolar membrane vesicles of *Saccharomyces cerevisiae*. *J Bacteriol* **180**: 1962–1965.

Parrou JL & François J (1997) A simplified procedure for a rapid and reliable assay of both glycogen and trehalose in whole yeast cells. *Anal Biochem* **248**: 186–193.

Philpott CC & Protchenko O (2008) Response to iron deprivation in *Saccharomyces cerevisiae*. *Eukaryot Cell* **7**: 20–27.

Puig S, Askeland E & Thiele DJ (2005) Coordinated remodeling of cellular metabolism during iron deficiency through targeted mRNA degradation. *Cell* **120**: 99–110.

Reck BK, Müller DB, Rostkowski K & Graedel TE (2008) Anthropogenic nickel cycle: insights into use trade and recycling. *Environ Sci Technol* **42**: 3394–3400.

Robinson MD, Grigull J, Mohammad N & Hughes TR (2002) FunSpec: a web-based cluster interpreter for yeast. *BMC Bioinformatics* **3**: 35.

Ruepp A, Zollner A, Maier D *et al.* (2004) The FunCat, a functional annotation scheme for systematic classification of proteins from whole genomes. *Nucleic Acids Res* **32**: 5539–5545.

Ruotolo R, Marchini G & Ottonello S (2008) Membrane transporters and protein traffic networks differentially affecting metal tolerance: a genomic phenotyping study in yeast. *Genome Biol* **9**: R67.

Russek E & Colwell RR (1983) Computation of most probable numbers. *Appl Environ Microbiol* **45**: 1646–1650.

Rutherford JC, Ojeda L, Balk J, Mühlenhoff U, Lill R & Winge DR (2005) Activation of the iron regulon by the yeast Aft1/Aft2 transcription factors depends on mitochondrial but not cytosolic iron-sulfur protein biogenesis. *J Biol Chem* **280**: 10135–11040.

Sauer U (2001) Evolutionary engineering of industrially important microbial phenotypes. *Adv Biochem Eng Biotechnol* **73**: 130–166.

Schmittgen TD & Livak KJ (2008) Analyzing real-time PCR data by the comparative C_T method. *Nat Protoc* **3**: 1101–1108.

Şen M, Yılmaz Ü, Baysal A, Akman S & Çakar ZP (2011) *In vivo* evolutionary engineering of a boron-resistant bacterium: *Bacillus boroniphilus*. *Antonie Van Leeuwenhoek* **99**: 825–835.

Stadler JA & Schweyen RJ (2002) The yeast iron regulon is induced upon cobalt stress and crucial for cobalt tolerance. *J Biol Chem* **277**: 39649–39654.

Stearman R, Yuan DS, Yamaguchi-Iwai Y, Klausner RD & Dancis A (1996) A permease-oxidase complex involved in high affinity iron uptake in yeast. *Science* **271**: 1552–1557.

Takumi S, Kimura H, Matsusaki H, Kawazoe S, Tominaga N & Arizono K (2010) DNA microarray analysis of genomic responses of yeast *Saccharomyces cerevisiae* to nickel chloride. *J Toxicol Sci* **35**: 125–129.

Valko M, Morris H & Cronin MTD (2005) Metals, toxicity and oxidative stress. *Curr Med Chem* **12**: 1161–1208.

Wisselink HW, Toirkens MJ, Wu Q, Pronk JT & van Maris AJ (2009) Novel evolutionary engineering approach for accelerated utilization of glucose xylose and arabinose mixtures by engineered *Saccharomyces cerevisiae* strains. *Appl Environ Microbiol* **75**: 907–914.

Yamaguchi-Iwai Y, Dancis A & Klausner RD (1995) AFT1: a mediator of iron regulated transcriptional control in *Saccharomyces cerevisiae*. *EMBO J* **4**: 1231–1239.

Yasokawa D & Iwahashi H (2010) Toxicogenomics using yeast DNA microarrays. *J Biosci Bioeng* **110**: 511–522.